Understanding and control of the metallic state in epitaxial NdNiO3

Guo, Qikai

DOI:
10.33612/diss.180302851

Chapter 6

The intermediate metallic character of epitaxial nickelates

Prompted by the discovery of superconductivity in the infinite-layer nickelates, a deeper understanding of the metallic behaviour of the $NdNiO_3$ (NNO) is needed. In the present work, we unveil that a cuprate-like linear-T-resistivity is maintained in the NNO films over a wide temperature range (100-550 K); while the resistivity shows a clear deviation from the linear trend at higher temperature, consistent with the addition of a parallel saturation channel. Detailed analysis of the structural and electrical properties reveals that the resistivity of pristine NNO films (pure phase, low strain, and weak interfacial effects) does obey the Mott-Ioffe-Regel limit, thus lacking the signatures of bad metal behaviour. In order to deal with the ambivalent nature of the metallic state in nickelates and other electron correlated systems, we propose to classify metals simply on the basis of the strength of the electron scattering. In this way, nickelates are shown to belong to a distinct regime of moderate scattering, intermediate between those of normal metals and bad metals. This explains the combination of strange metallicity and conventional behaviour observed in these systems and clarifies existing controversies.

6.1 Introduction

Many materials with strong electron correlations show puzzling metallic behaviour, posing challenges to our conventional understanding of metals on the basis of coherent quasiparticles (CQP) [1–6]. This class of materials includes the "strange metals", for which the resistivity follows an anomalous linear dependence with temperature (T) at T values sufficient low for the Fermi liquid description (T^2) to be dominant; and the "bad metals", for which the resistivity crosses the Mott-Ioffe-Regel (MIR) bound at high-T, implying such large scattering rates that, according to Heisenberg's principle, the uncertainty in the quasi-particle energy must exceed the coherence regime, thus, disqualifying the quasi-particle description.

Understanding these behaviours has become one of the central tasks in condensed matter physics and has energized the emergence of several new concepts

in recent years. For instance, in many strange metallic systems, such as the ruthenates [2], cuprate superconductors [7], and heavy fermions [8], the T-linear resistivity was found to share a similar "*Planckian dissipation*". This recent concept emphasizes that the T-linear resistivity can be obtained as long as the scattering rate per kelvin of charge carries reaches a universal bound, $k_B/\hbar$, [1, 2, 7], regardless of their distinct scattering mechanism (electron-phonon, electron-electron scattering, etc) and different strength of electron correlations.

As perovskites with strong electron-correlations, rare-earth nickelates ($RENiO_3$) have also been discussed as a system with bad metallicity by Jaramillo *et al* [9]. However, successive works put forward an alternative suggestion in which the resistivity of nickelates does saturates below the MIR limit [10–12], supporting the validity of the quasi-particle carrier scenario in this material's family. These contradictory results may arise from the large tunability of resistivity in nickelates. The metallicity of nickelates is mainly determined by the overlap between Ni e_{g} and O $2p$ orbitals; however, this overlap shows an extreme sensitivity to the minor change in the local lattice [13]. In this case, epitaxial strain and lattice imperfections have been revealed to modify the value of resistivity in nickelate thin films [10, 14–17]. Recently, also the scaling exponent of the resistivity-T dependence in the metallic phase has been shown to systematically change with the oxygen vacancy content[18, 19]. Notably, these modified resistivities in the intermediate temperature range can raise serious difficulties in the estimation of an intrinsic saturation resistivity (ρ_{SAT}), especially, when the temperature range of the resistivity measurements is limited.

In the present work, thin films of $NdNiO_3$ (NNO) were epitaxially grown on $LaAlO_3$ substrates. Detailed analysis reveals a pure phase and negligible effect of strain and lattice defects on the resistivity for films with thickness below 10 nm. Unconventional measurements in an extended temperature range (up to 700 K), indicate that the resistivity of nickelate films indeed shows saturation when the electronic mean-free-path becomes comparable with the atomic distance. We also demonstrate that interfacial effects are at play in determining the value of ρ_{SAT}, especially in ultra-thin films. The comparison of our NNO films with other metallic systems, including conventional metals, bad metals, and strange metals, manifests that the resistivity of $RENiO_3$ and several other metallic systems is likely located in an intriguing intermediate region between conventional metals and bad metals, casting questions on their common origin and appealing for further works to fully understand this behaviour.

6.2 Methods

High quality epitaxial $NdNiO_3$ thin films were deposited on single-crystal $LaAlO_3$ (LAO) substrates by pulsed laser ablation of a single-phase target (Toshima Manufacturing Co., Ltd.). Before deposition, the LAO substrates were thermal annealed at 1050 °C in a flowing O_2 and etched by DI water to obtain an atomically flat surface with single termination terraces. During the deposition, the substrates were heated to a high temperature 700 °C and then the films were uniformly deposited on the substrates. The applied oxygen pressure was 0.2 mbar and the laser fluence on the target was 2 J/cm^2. After deposition, the samples were cooled down to room temperature at 5 °C/min. Films with various thicknesses had been grown by precisely tuning the deposition time as the deposition rate was constant.

Following growth, the structural and transport properties of all films were carefully studied in detail. The thicknesses of all films were detected using X-ray diffraction. Cross-sectional specimens of the films were prepared and studied by scanning transmission electron microscopy (STEM) on a probe corrected FEI Titan 60–300 microscope equipped with a high-brightness field emission gun (X-FEG) and a CEOS aberration corrector for the condenser system. This microscope was operated at 300 kV. High angle annular dark field (HAADF) STEM images were acquired with a convergence angle of 25 mrad and a probe size below 1 Å. The strain state of the films was determined by geometrical phase analysis (GPA) of these HAADF images.

The temperature dependence of resistivity under room temperature were carried out in a van der pauw symmetry using a Quantum design physical property measurement system (PPMS), while those measurements above room temperature were performed on a Instec probe station. AC measurement was performed using a LCR Agilent E4980.

6.3 Results

Stoichiometric NNO films with pure phase have been grown by pulsed laser deposition (PLD) on LAO substrates, using a single-phase ceramic target. The negligible mismatch between NNO and LAO (-0.3 %) yields a almost strain-free lattice of films. After deposition, the samples were slowly cooled down to room temperature with a high oxygen pressure (900 mbar) to avoid the formation of oxygen vacancies in the lattice. The crystalline structure of films were studied by atomic resolution scanning transmission electron microscopy (STEM). As shown in Fig. 6.1(a) and (b), the cross-sectional HAADF-STEM images indicate a high crystalline quality in both the 2 nm and 10 nm NNO films grown on LAO substrates. Clearly, the images evidence a very good crystalline quality. No misfit dislocations or other common defects such

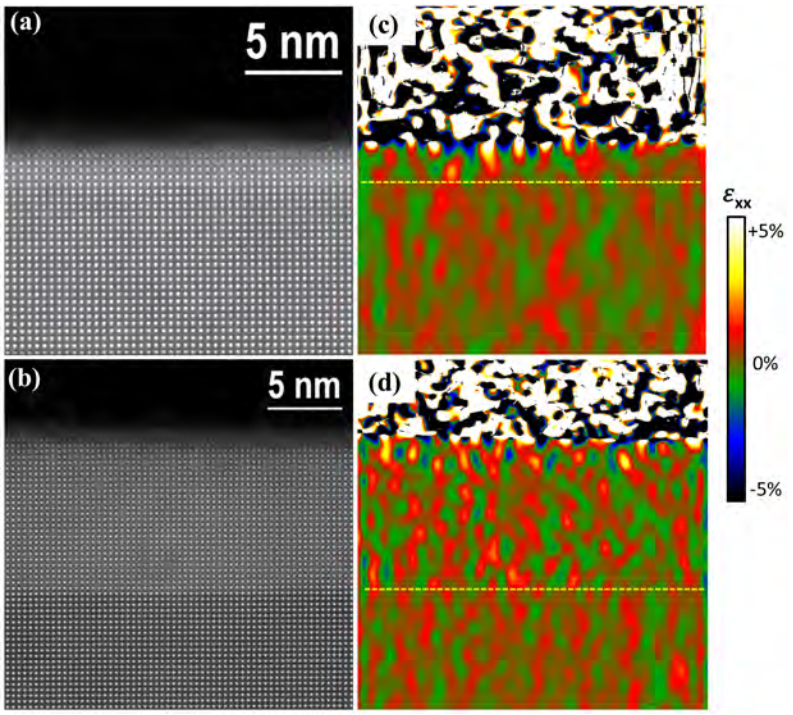

Figure 6.1: *Cross-sectional HAADF-STEM image of 2 nm (a) and 10 nm (b) $NdNiO_3$ thin film grown on a $LaAlO_3$ substrates. The respective in-plane components of the strain tensor (ϵ_{xx}, colour scales) obtained from the STEM images by geometrical phase analysis (GPA) are shown in (c) and (d).*

as Ruddlesden-Popper (PR) faults, which are known to form in nickelates in the presence of excess A-cations or oxygen vacancies, are observed in the lattice. As revealed in our previous work, the thickest NNO film grown on LAO substrate that can keep a pure perovskite phase is 10 nm, above which the PR faults usually appear [18]. Similar phenomenon has also been reported by Lee $at\ al$ [20] and was found to be crucial for the reduction and stabilization of superconducting infinite-layer phase in the same material. In this sense, all films investigated here are thinner than this critical thickness to minimize the affect of lattice disorder, which is believed to have a robust influence on the transport performance of this material [9, 10, 21].

The components of the strain tensor in the in-plane direction of the films shown in Fig. 6.1(a) and (b) was also obtained by geometrical phase analysis (GPA). From Fig. 6.1(c), it is clear that the deformation of in-plane lattice parameter respect to substrate (ε_{xx}) in 2 nm film is of the order of the typical noise of the technique, giving

a homogeneous strain in the films with a average value near to zero, and manifesting a coherent growth of film under strain-free conditions. With further increase of film thickness, the coherence of in-plane lattice parameter is still maintained up to 10 nm (see Fig. 6.1(d)), eliminating eliminating strain relaxation as a possible effect on the electrical transport properties discussed below.

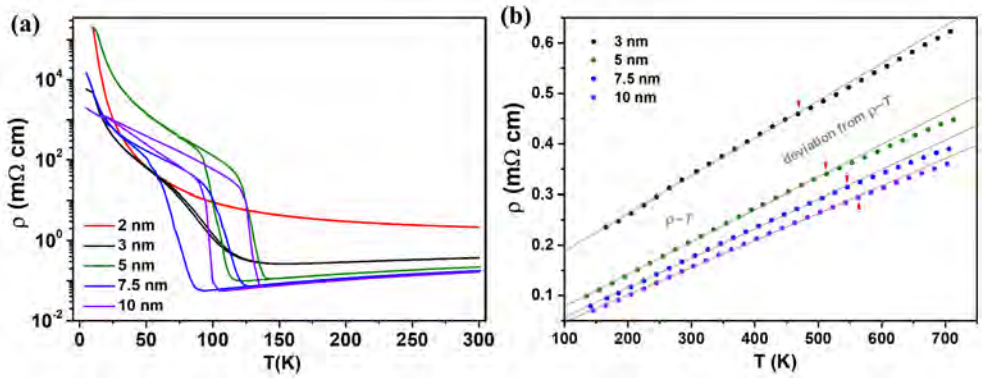

Figure 6.2: *(a) The resistivity of NNO/LAO films with different thickness as a function of temperature. (b) Extended resistivity till to 700 K in the metallic phase of NNO/LAO films. The solid lines represent the linear fits to the ρ(T) data; while the red arrows indicate the deviation of ρ(T) from the linear-dependence.*

Fig. 6.2(a) shows the temperature-dependent resistivity (ρ(T)) of NNO films from 5 K to 300 K. Clearly, a first-order transition from high-T metal to a low-T insulator with characteristic hysteresis can be observed in all films with thickness above 5 nm; whilst the metal-insulator transition (MIT) becomes less robust in ultra-thin films. For instance, the hysteresis is nearly unrecognizable in the 3 nm film and, eventually, the MIT is fully suppressed in the ultra-thin 2 nm one, which is usually attributed to the modified electronic structures at the interface and surface [22, 23].

Another intriguing feature of these pristine specimens is a linear-T-resistivity characteristic of strange metallicity. As discussed in our previous work [18, 19], this T-linear behaviour of resistivity can only be achieved in optimized NNO films with low oxygen vacancy content and, more interestingly, it has the signatures of Planckian-like dissipation ($1/\tau \simeq k_B T/\hbar$) [19]. In order to further investigate the robustness of this behaviour, we performed extended measurement of resistivity up to 700 K. The corresponding results, merged with the metallic resistivity data below 300 K, shown in Fig. 6.2(a), were plotted in Fig. 6.2(b). Notably, the linear temperature dependence of resistivity in all of these NNO/LAO films, despite of their distinct thickness and T_{MI}, survives in a ultra-wide temperature range (over 400 K). It is worth noting that the reported value of Debye temperature in nickelates is 420

K [24]. Therefore, this robust linear-T-resistivity is maintained from low-T to high-T across the Debye temperature, pointing to an origin of the linear resistivity independent of the type of electron interactions, as established by the Planckian dissipation concept [2].

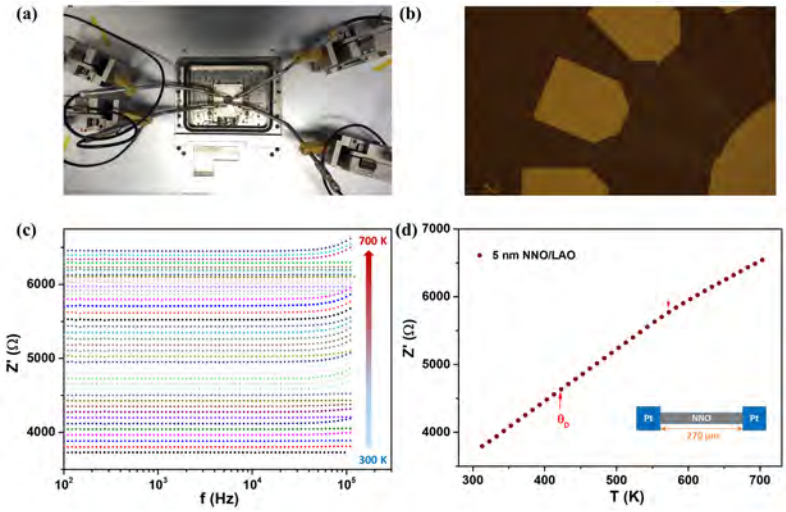

Figure 6.3: *(a) To-view of the custom-made probe station with high temperature Thermo chuck. (b) Geometry of the device. AC measurement was performed between two terminals of a NNO bridge with a size of 270 μm $\times$ 50 μm. (c) Frequency dependence of the real part of the complex impedance for a 5 nm NNO film grown on a LAO substrate. (d) The real part of the impedance as a function of temperature. The red arrow indicates the reported Debye temperature in nickelates.*

With the further increase of T, the rise of ρ(T) in all the NNO/LAO films (with thickness above 2 nm) shows an obvious deviation from the linear dependence, which can be characterized by the substantially reduced slope in Fig. 6.2(b) above 500 K (deviations from linearity larger than 1.0 $\%$ are indicated with blue arrows). This behaviour is consistent with a saturation of the resistivity at high temperatures. To eliminate the effect of electrode contacts, electrode-film interface and other possible artifacts, we also performed an AC measurement between two terminals of a NNO bridge with a size of 270 $\mu m \times 50$ μm (see Fig. 6.3). As shown in Fig. 6.3(d), the real part of the impedance (resistance) also shows a similar deviation from the original linear-T dependence at a similar temperature ($\sim$550 K) compared with that of the DC measurements in Fig. 6.2(b). This observed offset of linear scaling and saturation of resistivity can be described by the addition of a parallel resistance that takes over the behaviour in the high temperature regime [25, 26], as the electron mean-free-path

(ℓ) gradually approaches the interatomic distances of the film. However, the possible effect of structural changes, such as a phase transition from orthorhombic phase to rhombohedral or cubic phase, should also be discarded.

6.3.1 Absence of structural anomalies at high temperatures

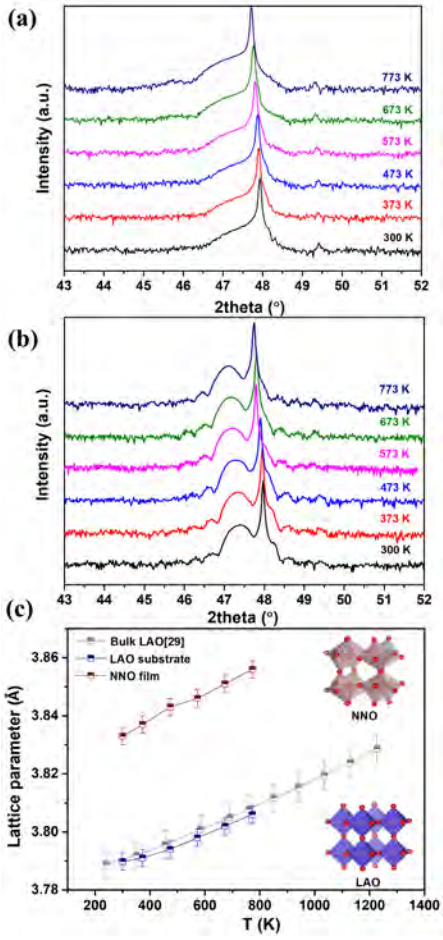

Figure 6.4: *2θ-ω scannings around the LAO (002) peak for (a) 10 nm and (b) 20 nm NNO/LAO film at various temperature. (c) The extracted out-of-plane lattice parameters for both the NNO film and the LAO substrate as a function of temperature.*

To gain structural insight into the observed offset of resistivity, 2θ-ω scannings around the NNO $(002)_{pc}$ peak were performed at various temperature. As shown in

Fig. 6.4 (a), the LAO substrate shows a sharp $(002)_{pc}$ peak, while the 10 nm NNO films (the thickest one investigated in Fig. 6.2) only display a broad peak as a shoulder of the substrate peak because of their small thickness and small lattice mismatch with LAO. With the rise of temperature, the LAO $(002)_{pc}$ peaks shift gradually to smaller angles from 47.93° (300 K) to 47.71° (773 K), which corresponds to an extension of lattice parameter from 3.79 Å to 3.81 Å. However, despite the visible shift of the peak, a direct extraction of the c for the NNO film is challenging in this thickness due to the absence of an intact film peak. Therefore, comparable 2θ-ω scans on a 20 nm NNO/LAO film, which shows a separated film peak, were employed to track the out-of-plane lattice parameter of NNO films at various temperatures with higher accuracy. From Fig. 6.4(b), it is clear that the $(002)_{pc}$ peak of the NNO film and the LAO substrate are indeed shifted to smaller angle with the increasing temperature, as expected from thermal expansion. A quantitative analysis of the lattice parameter for both the NNO film and LAO substrate is shown in Fig. 6.4(c). For comparison, the reported values of bulk LAO in an extended temperature were also plotted [27]. The increase of interatomic spacing in the LAO substrate with temperature is well consistent with reported values [27]. As revealed by Hayward $et\ al.$, a structural transition from rhombohedral phase to cubic phase can happen in LAO at 850 K. In the nickelates, only $PrNiO_3$ has shown a transition at 773 K from an orthorhombic (*Pbnm*) to a rhombohedral ($R\bar{3}c$) phase [28]). However, these temperatures are far beyond the range where the resistivity starts to deviate from the linear-T dependence, ruling out their roles in explaining the observations.

6.3.2 Saturation resistivity

According to Boltzmann's theory, the carrier mean free path, ℓ, decreases with increasing temperature due to the profusion of scattering events. However, as argued by Ioffe and Regel based on the uncertainty principle, in a quasiparticle description of the metallic state, ℓ can never become smaller than the interatomic distance (of the order of the lattice parameter, a) [29]. Thus, discarding structural effects, the most plausible explanation is that what we observe in Fig. 6.2(b) is the start of resistivity saturation to comply with the MIR limit. In order to establish if this is the case, we estimate the temperature dependence of ℓ in our NNO films from the resistivity data by using

$$\rho = \frac{3\pi^2\hbar}{e^2 k_F^2 \ell} \tag{6.1}$$

where e is the elementary charge, $\hbar$ is the reduced Planck constant, and k_F is the Fermi wavevector, which can be approximately estimated from the carrier density (n) by $k_F = (3\pi^2 n)^{1/3}$ in 3D system.

Herein, a theoretical value $\sim 10^{22}$ cm^{-3} was adopted as the total carrier density of NNO films by assuming 1 carrier per Ni, which is common practice [10–12], given the difficulties to interpret the Hall measurements in these materials [19]. For comparison, the extracted values of ℓ are plotted in Fig. 6.5(a) together with the (out-of-plane) lattice parameters of the NNO film at various T (from Fig. 6.5(c)). As shown in Fig. 6.5(a), the ℓ of electrons in all the films displays a dramatic decrease with the increasing temperature at lower T (below 500 K); while it shows a sign of saturation at high-T, when its value becomes 1-3 times larger than the lattice parameter. This strongly suggests that the offset of the linear-ρ(T) in Fig. 6.2 (b) arises from the proximity to the MIR limit.

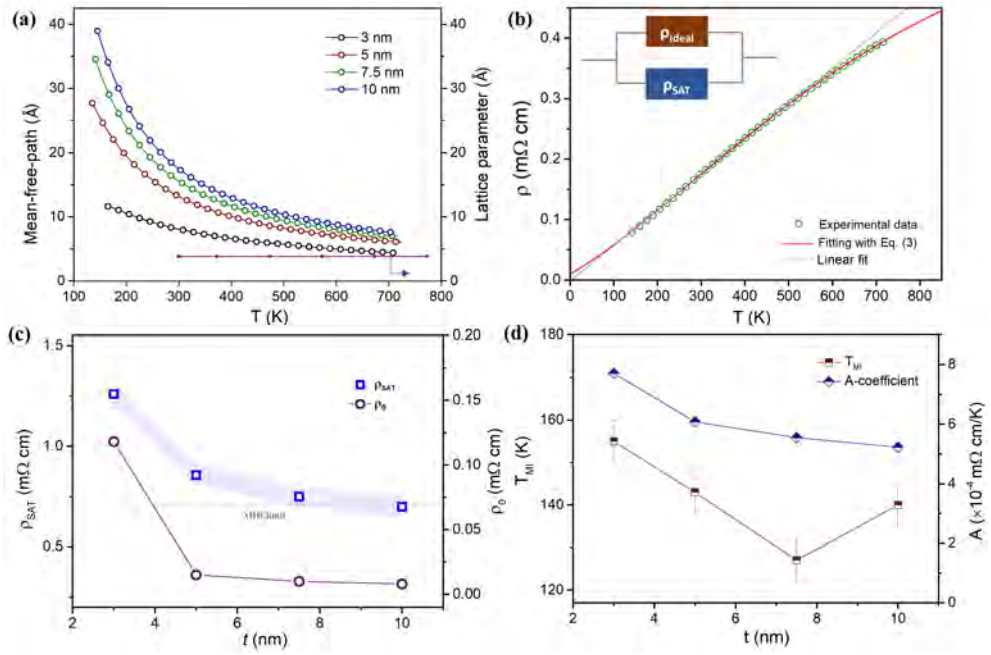

Figure 6.5: *(a) Extracted mean-free-path (ℓ) from the resistivity data as a function of temperature. The red line points to a temperature dependence of lattice parameter in a NNO/LAO film. (b) The fit of ρ(T) with the parallel resistor model illustrated in Eq. 6.2, accompanied with a linear fit. (c) The extracted ρ_{SAT} and ρ_0 as a function of thickness. The gray dashed line indicates the MIR limit in NNO. (d) Thickness-dependence of the A-coefficient and the T_{MI} in NNO/LAO films.*

However, a direct measurement of ρ_{SAT} is still far beyond the scope of our set-up and may be too high to keep the film integrity or even be higher than the melting temperature of nickelates, as in most of other conventional metals. Alternatively, a

fitting of the resistivity curve in the available temperature range is extrapolated to ultra-high temperatures. As revealed by previous works with other electron correlated systems [25, 26, 30], also in the case of nickelates we can show that the T-dependence of the saturating resistivity can be well fit to a so-called "parallel-resistor" model:

$$\rho(T)^{-1} = \rho_{\text{ideal}}(T)^{-1} + \rho_{\text{sat}}{}^{-1} \tag{6.2}$$

where ρ_{ideal} is the ideal resistivity in the absence of saturation, which is shunted by the large value of ρ_{SAT} at high temperature. Note that one of the key challenges in the fit is how to define ρ_{ideal}. One proposal for this is a model, in which ρ_{ideal} follows a simple linear-T dependence (ρ_{ideal}=ρ_0+AT). Indeed, although, as d-band perovskite oxides, rare-earth nickelates should display strong electron correlations, the Plankian-like dissipation observed in NNO/LAO films, starting from temperatures well below the Debye temperature, gives rise to strange-metal-like linear-T-resistivity. However, extrapolating the linear fit to low temperatures gives rise to an unphysical negative residual resistivity (see Fig. 6.2(b)), which indicates the need to add a Fermi-liquid term to the fit. We then can propose a dual-component model, similar to that used by Hussey et al. in high-T_{C} cuprates [31, 32], in order to describe ρ_{ideal} as:

$$\rho_{\text{ideal}}(T) = \rho_0 + AT + BT^2 \tag{6.3}$$

where ρ_0 represents the residual resistivity, while A and B characterize the strength of electron scattering from various contributions (e.g. electron-phonon or electron-electron scattering). Then, the total resistivity in the metallic state of the films can be estimated by replacing the ρ_{ideal} in Eq. 6.2 with Eq. 6.3.

An example of the fit is shown in Fig. 6.5(b). Notably, the value of ρ_{SAT} in these thin films displays a sharp increase with decreasing film thickness and stays almost constant for thickness beyond 7.5 nm. Similar evolution is also observed in the thickness-dependence of ρ_0. Since ρ_0 represents the scattering of electrons by lattice defects and the HAADF-STEM images shown in Fig. 6.1 reveal that all the investigated films in this work show similar crystal quality, we can associate the dramatic increase of ρ_0 in thinner films with interface/surface scattering. In the ultra-thin 2 nm film, the interfacial effects become even more crucial and compel the film to behave as a semiconductor in the whole temperature range.

6.4 Discussion

Let us now discuss the effect of interface on the electronic structure of nickelates. As shown in Fig. 6.5(d), the T_{MI} of NNO films shows a robust increase with reduced

thickness. It is worth to note that the relaxation of epitaxial strain with thickness cannot explain this variation in T_{MI}, as the strain relaxation in our NNO/LAO system happens for thicknesses larger than 40 nm [18]. In addition, the strain relaxation should yield an opposite trend of T_{MI}, increasing toward its bulk counterpart (200 K in bulk NNO [33]). Moreover, the GPA analysis on the STEM images (see Fig. 6.1) also points to a negligible ε_{xx} in all the investigated films. Instead, interfacial effects, such as orbital polarization, electronic reconstruction, and the rearrangement of octahedral rotations under the influence of the substrate, should be considered.

In $RENiO_3$, two Ni e_{g} bands with symmetry x^2-y^2 and $3z^2$-r^2 cross the Fermi level [10]. In the bulk nickelates, these two bands are degenerate. The application of epitaxial strain was found to give rise to an orbital polarization with preference for the x^2-y^2 orbitals in the films with tensile strain and preference for the $3z^2$-r^2 orbitals in the compressive films [10, 34], as shown in Fig. 6.6(a). More interestingly, density functional theory (DFT) calculations by Mikheev *et al.* revealed that this orbital polarization in the Ni e_{g} band shows a cogent correlation with the ρ_{SAT} in nickelates [10]. In our case, the strain is unchanged. However, Peng *et al.*[35] reported that orbital polarization can also be promoted with the decrease of film thickness. This could explain the observed lifting in the ρ_{SAT}.

The difference in electronic properties and structural symmetries between the rhombohedral LAO substrate and the orthorhombic NNO film should also exert an effect on the resistivity, especially for the thinner films. Liu *et al.* argued that the distinct properties between LAO and nickelates in both the electronegativity and electronic configurations create a strongly-modified electronic structure at the interface of nickelate thin films [36]. This is well consistent with a fully suppressed metallic phase in the 2 nm NNO/LAO films, most likely due to the influence of the substrate over the entire layer. Moreover, the coherent growth should also create a rearrangement of the octahedral network in the NNO films to maintain a connectivity with the LAO substrate at the interface [37, 38]. As a result, the $a^-a^-c^+$ tilt pattern, which is dominant in the orthorhombic phase of nickelates, was found to be quenched in the epitaxial NNO film grown on LAO substrate ($a^-a^-a^-$) [37]. Similar suppression of octahedral rotations was also reported in the NNO/$SrTiO_3$ superlattices [38]. In both cases, the changes in the octahedral tilt pattern were revealed to alter the electronic properties of NNO films.

As discussed in Chapter 3, we found a set of half integer reflections (marked with yellow circles) present in the 10 nm film; while these reflections are absent for 5 nm film. Simulated electron diffraction patterns of bulk LAO and NNO revealed that these half integer reflections also disappear in rhombohedral LAO but become robust in the orthorhombic NNO. These results, therefore, suggest that the change of the in-plane tilt of NiO_6 octahedra in the thinner film is yielded by the LAO substrates. On the contrary, the recovery of the in-plane octahedral titling in the 10 nm

NNO film manifests a full decoupling from the interfacial effects at this thickness, which is consistent with its lower ρ_0 and increase of T_{MI} shown in Fig. 6.5 (c) and (d).

6.4.1 Good metal or bad metal

At last, we discuss the possible bad-metallic behaviour in these NNO films. According to the scenario of Ioffe and Regel, the MIR limit (ρ_{MIR}) can be simply estimated by replacing ℓ with a in Eq. (6.1) [29]. Then, metals that display a resistivity across this limit are recognized as bad metals; otherwise, they are considered as conventional metals. The corresponding value of ρ_{MIR} for nickelates is marked in Fig. 6.5(c). Notably, the NNO films studied in this work show a surprising crossover from bad metal to conventional metal with the increase of thickness, when the interfacial effects described above become negligible. In previous works [10–12], epitaxial strain, Cu doping, and oxygen deficiency, have been found to modify the value of ρ_{SAT} in nickelates. For instance, the NNO films were reported to satisfy the MIR scheme when the strain is small; while an enhanced value of ρ_{SAT} was observed in the same compound with large strain [10]. In the current work, we show that interfacial effects (e.g orbital polarization and octahedral rearrangement) also plays a crucial role in determining the ρ_{SAT} even in the pure and nearly strain-free case.

We, therefore, show that for the NNO/LAO system, the 10 nm thick films represent the intrinsic behaviour of NNO films for several reasons: 1) these films are nearly strain-free, as all the other films on LAO substrates; 2) the recovered in-plane c^+ octahedra rotations and the small ρ_0 suggests a disengagement from the interfacial effects at this thickness; 3) they exhibit a pure phase (PR faults are not yet present at this thickness [18, 20]). Therefore, the influence of epitaxial strain, lattice defects, and interfacial effects, on the electrical transport properties can be mostly neglected in this thickness. The validity of the MIR scenario ($\rho_{\mathrm{SAT}} \leq \rho_{\mathrm{MIR}}$) in the 10 nm NNO films then manifests that the nickelates are intrinsically not bad metals. This conclusion is re-enforced when an alternative scenario is employed to estimate the MIR limit from the expression, $k_{\mathrm{F}}\ell$=1. In the 2D form, the $k_{\mathrm{F}}\ell$ is related to the sheet resistance ($R_{\square}$) of the film by:

$$k_{\mathrm{F}}\ell = \frac{h/e^2}{R_{\square}} = \frac{25k\Omega/\square}{R_{\square}} \tag{6.4}$$

As shown in Fig. 6.6(c), the $k_{\mathrm{F}}\ell$ of all the films (even the 3 nm one) is far from unity.

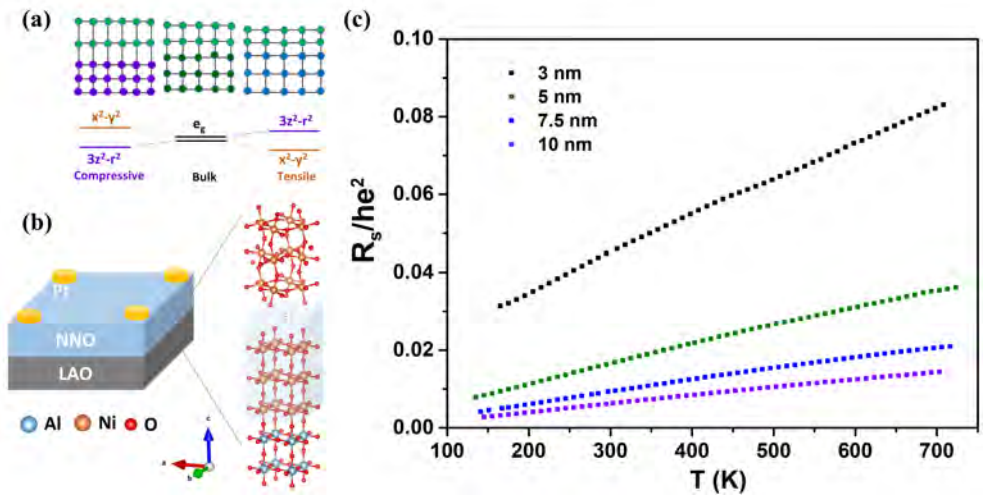

Figure 6.6: *(a) Schematic illustrates the orbital polarization in NNO film with different strain conditions. (b) A sketch represents the geometric structure of the NNO/LAO device and the evolution of the octehedral rotation mode with the increasing thickness. (c) Normalized 2D resistivity in the unit of h/e^2 for NNO/LAO films with various thickness.*

6.4.2 Intermediate strength of electron scattering

In Figure 6.7, we present the ρ(T) curves of various metals, including conventional metals, bad metals, and our NNO/LAO film, in one plot. Compared with the slowly increased resistivity of conventional metals (e.g Cu, Nb, and Nb_3Sb, in the red region), the slope of ρ(T) in those well-known bad metals (in the blue region) is ultra-large, as expected from strong electron scattering. As a result, the resistivity can cross the MIR limit at relatively low temperatures and approach a value far beyond the ρ_{MIR} at high temperatures, violating the quasiparticle scenario, and earning them the bad metal character.

However, there are also some electron correlated metals located in the intermediate region (between blue and red regions). These metallic systems, with resistivity slopes ranging from about 0.1 $\mu\Omega$ cm/K^{-1} to 1 $\mu\Omega$ cm/K^{-1} are interesting because they possess properties of both conventional metals and bad metals. For instance, Sr_2RuO_4 was believed to be a very conventional metal according to their low-T Fermi-liquid-like performance of resistivity [48]; however, it shows no sign of saturation till 1300 K, suggesting a bad metallic behaviour [46]. Other metallic compounds, such as chromium dioxide (CrO_2) [49], show signs of saturation but at higher values than that predicted by the MIR scenario. Notably, the resistivities of nickelate films (e.g $SmNiO_3$ [9] and NNO) are also located in this intermediate region. This can be

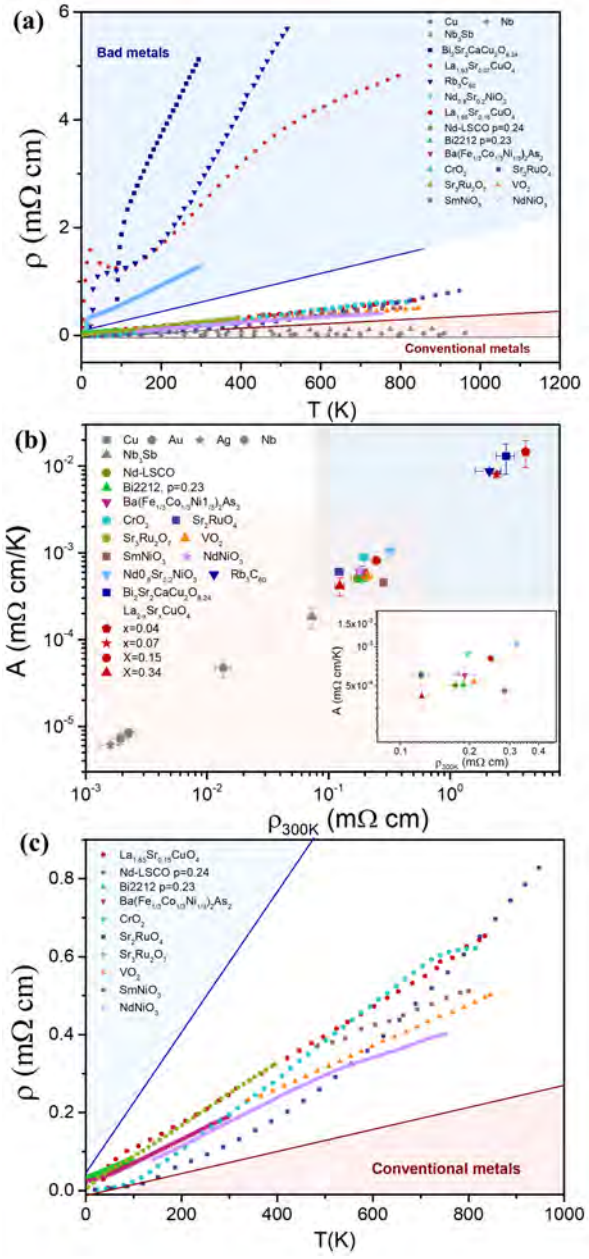

Figure 6.7: *Summary of resistivity for various metals. (Data source: Cu, Nb, Nb_3Sb [39], $Nd_{0.8}Sr_{0.2}NiO_2$ [40], $La_{2-x}Sr_xCuO_4$ [41], Rb_3C_{60} [42], $Bi_2Sr_2CaCu_2O_{8.24}$ [43], Nd-LSCO (p=0.24) and Bi2212 (p=0.23) [7], $Ba(Fe_{1/3}Co_{1/3}Ni_{1/3})_2As_2$ [44], CrO_2 [45], Sr_2RuO_4 [46], $Sr_3Ru_2O_7$, [2], VO_2 [47], $SmNiO_3$ [9].)*

more clearly seen in Fig. 6.7(b) where both the A-coefficient and, correlated to that, the ρ(300K) of nickelate films, show intermediate values between conventional metals and other strongly correlated metals. In this sense, it is not surprising that the definition of this material as bad metal or conventional metal becomes controversial [9, 10].

Metallic systems located in this intermediate regime, become even more interesting as some of them (see Fig. 6.7(c)), such as $La_{2-x}Sr_xCuO_4$ [50], Nd-LSCO (p=0.24) and Bi2212 (p=0.23) [7], $Ba(Fe_{1/3}Co_{1/3}Ni_{1/3})_2As_2$ [44], and $Sr_3Ru_2O_7$ [2], are found to satisfy a universal "*Planckian dissipation*" ($1/\tau \simeq k_B T/\hbar$) [1, 2, 7]. This recent concept has received great interest as it may be key in understanding the puzzling origin of the linear-T-resistivity in high-T_c superconductors and other electron-correlated systems. Interestingly, the values of A obtained for different types of superconductors, shown to be correlated to the the magnitude of T_c and tuned by means of doping, pressure or compositions [51] also belong to this mid-A region.

To conclude, extended measurement up to high temperatures in NNO films with low strain, pure phase and negligible interfacial effects, reveal that the robust linear-T-resistivity, which is dominant in a wide intermediate T range, saturates at high temperature, fulfilling the MIR limit. Therefore, we conclude that pristine NNO films are not bad metals. If metals are simply classified by the strength of the electron scattering, nickelates and various other strongly correlated electron systems belong to an intermediate scattering regime distinct from both bad and normal metals.

Bibliography

[1] J. Zaanen, "Planckian dissipation, minimal viscosity and the transport in cuprate strange metals," 2019.

[2] J. Bruin, H. Sakai, R. Perry, and A. Mackenzie, "Similarity of scattering rates in metals showing T-linear resistivity," *Science* **339**(6121), pp. 804–807, 2013.

[3] S. A. Hartnoll, "Theory of universal incoherent metallic transport," *Nature Physics* **11**(1), pp. 54–61, 2015.

[4] E. W. Huang, R. Sheppard, B. Moritz, and T. P. Devereaux, "Strange metallicity in the doped Hubbard model," *Science* **366**(6468), pp. 987–990, 2019.

[5] X. Deng, J. Mravlje, M. Ferrero, G. Kotliar, A. Georges, *et al.*, "How bad metals turn good: Spectroscopic signatures of resilient quasiparticles," *Physical review letters* **110**(8), p. 086401, 2013.

[6] P. T. Brown, D. Mitra, E. Guardado-Sanchez, R. Nourafkan, A. Reymbaut, C.-D. Hébert, S. Bergeron, A.-M. Tremblay, J. Kokalj, D. A. Huse, *et al.*, "Bad metallic transport in a cold atom Fermi-hubbard system," *Science* **363**(6425), pp. 379–382, 2019.

[7] A. Legros, S. Benhabib, W. Tabis, F. Laliberté, M. Dion, M. Lizaire, B. Vignolle, D. Vignolles, H. Raffy, Z. Li, *et al.*, "Universal T-linear resistivity and Planckian dissipation in overdoped cuprates," *Nature Physics* **15**(2), pp. 142–147, 2019.

[8] H. v. Löhneysen, T. Pietrus, G. Portisch, H. Schlager, A. Schröder, M. Sieck, and T. Trappmann, "Non-Fermi-liquid behavior in a heavy-fermion alloy at a magnetic instability," *Physical review letters* **72**(20), p. 3262, 1994.

[9] R. Jaramillo, S. D. Ha, D. Silevitch, and S. Ramanathan, "Origins of bad-metal conductivity and the insulator–metal transition in the rare-earth nickelates," *Nature Physics* **10**(4), p. 304, 2014.

[10] E. Mikheev, A. J. Hauser, B. Himmetoglu, N. E. Moreno, A. Janotti, C. G. Van de Walle, and S. Stemmer, "Tuning bad metal and non-Fermi liquid behavior in a Mott material: Rare-earth nickelate thin films," *Science advances* **1**(10), p. e1500797, 2015.

[11] E. Yadav, S. Harisankar, K. Soni, and K. Mavani, "Influence of Cu doping and thickness on non-Fermi liquid behaviour and metallic conductance in epitaxial $PrNiO_3$ thin films," *Applied Physics A* **124**(9), p. 614, 2018.

[12] S. Harisankar, K. Soni, E. Yadav, and K. R. Mavani, "Strain-mediated effects of oxygen deficiency and variation in non-fermi liquid behavior of epitaxial $PrNiO_{3-\delta}$ thin films," *Journal of Physics: Condensed Matter* **31**(13), p. 135601, 2019.

[13] F. Serrano-Sanchez, F. Fauth, J. L. Martínez, and J. A. Alonso, "Experimental observation of monoclinic distortion in the insulating regime of smnio3 by synchrotron x-ray diffraction," *Inorganic chemistry* **58**(17), pp. 11828–11835, 2019.

[14] G. Catalan, "Progress in perovskite nickelate research," *Phase Transitions* **81**(7-8), pp. 729–749, 2008.

[15] S. Catalano, M. Gibert, J. Fowlie, J. Iniguez, J.-M. Triscone, and J. Kreisel, "Rare-earth nickelates $RNiO_3$: thin films and heterostructures," *Reports on Progress in Physics* **81**(4), p. 046501, 2018.

[16] S. Middey, J. Chakhalian, P. Mahadevan, J. Freeland, A. J. Millis, and D. Sarma, "Physics of ultrathin films and heterostructures of rare-earth nickelates," *Annual Review of Materials Research* **46**, pp. 305–334, 2016.

[17] A. Tiwari, C. Jin, and J. Narayan, "Strain-induced tuning of metal-insulator transition in $NdNiO_3$," *Applied physics letters* **80**(21), pp. 4039–4041, 2002.

[18] Q. Guo, S. Farokhipoor, C. Magén, F. Rivadulla, and B. Noheda, "Tunable resistivity exponents in the metallic phase of epitaxial nickelates," *Nature Communications* **11**(1), pp. 1–9, 2020.

[19] Q. Guo and B. Noheda, "From hidden metal-insulator transition to Planckian metal by tuning disorder in a nickelate," *arXiv preprint arXiv:2011.11535* , 2020.

[20] K. Lee, B. H. Goodge, D. Li, M. Osada, B. Y. Wang, Y. Cui, L. F. Kourkoutis, and H. Y. Hwang, "Aspects of the synthesis of thin film superconducting infinite-layer nickelates," *APL Materials* **8**(4), p. 041107, 2020.

[21] C. Wang, C.-H. Chang, A. Huang, P.-C. Wang, P.-C. Wu, L. Yang, C. Xu, P. Pandey, M. Zeng, R. Böttger, *et al.*, "Tunable disorder and localization in the rare-earth nickelates," *Physical Review Materials* **3**(5), p. 053801, 2019.

[22] H. Dulli, P. A. Dowben, S.-H. Liou, and E. W. Plummer, "Surface segregation and restructuring of colossal-magnetoresistant manganese perovskites $La_{0.65}Sr_{0.35}MnO_3$," *Physical Review B* **62**(22), p. R14629, 2000.

[23] A. S. Disa, A. B. Georgescu, J. L. Hart, D. P. Kumah, P. Shafer, E. Arenholz, D. A. Arena, S. Ismail-Beigi, M. L. Taheri, F. J. Walker, *et al.*, "Control of hidden ground-state order in $NdNiO_3$ superlattices," *Physical Review Materials* **1**(2), p. 024410, 2017.

[24] K. Rajeev, G. Shivashankar, and A. Raychaudhuri, "Low-temperature electronic properties of a normal conducting perovskite oxide ($LaNiO_3$)," *Solid state communications* **79**(7), pp. 591–595, 1991.

[25] O. Gunnarsson, M. Calandra, and J. Han, "Colloquium: Saturation of electrical resistivity," *Reviews of Modern Physics* **75**(4), p. 1085, 2003.

[26] N. Hussey||, K. Takenaka, and H. Takagi, "Universality of the Mott–Ioffe–Regel limit in metals," *Philosophical Magazine* **84**(27), pp. 2847–2864, 2004.

[27] S. Hayward, S. Redfern, and E. Salje, "Order parameter saturation in $LaAlO_3$," *Journal of Physics: Condensed Matter* **14**(43), p. 10131, 2002.

[28] T. Huang, W. Parrish, H. Toraya, P. Lacorre, and J. Torrance, "High-temperature crystal structures of orthorhombic and rhombohedral $PrNiO_3$," *Materials research bulletin* **25**(9), pp. 1091–1098, 1990.

[29] A. Ioffe and A. Regel, "Non-crystalline, amorphous and liquid electronic semiconductors,"

[30] N. Hussey, "The normal state scattering rate in high-cuprates," *The European Physical Journal B-Condensed Matter and Complex Systems* **31**(4), pp. 495–507, 2003.

[31] R. Cooper, Y. Wang, B. Vignolle, O. Lipscombe, S. Hayden, Y. Tanabe, T. Adachi, Y. Koike, M. Nohara, H. Takagi, *et al.*, "Anomalous criticality in the electrical resistivity of $La_{2-x}Sr_xCuO_4$," *Science* **323**(5914), pp. 603–607, 2009.

[32] N. E. Hussey, "Phenomenology of the normal state in-plane transport properties of high-T_c cuprates," *Journal of Physics: Condensed Matter* **20**(12), p. 123201, 2008.

[33] P. Lacorre, J. Torrance, J. Pannetier, A. Nazzal, P. Wang, and T. Huang, "Synthesis, crystal structure, and properties of metallic $PrNiO_3$: Comparison with metallic $NdNiO_3$ and semiconducting $SmNiO_3$," *Journal of Solid State Chemistry* **91**(2), pp. 225–237, 1991.

[34] D. Pesquera, G. Herranz, A. Barla, E. Pellegrin, F. Bondino, E. Magnano, F. Sánchez, and J. Fontcuberta, "Surface symmetry-breaking and strain effects on orbital occupancy in transition metal perovskite epitaxial films," *Nature communications* **3**(1), pp. 1–7, 2012.

[35] J. Peng, C. Song, M. Wang, F. Li, B. Cui, G. Wang, P. Yu, and F. Pan, "Manipulating the metal-to-insulator transition of $NdNiO_3$ films by orbital polarization," *Physical Review B* **93**(23), p. 235102, 2016.

[36] J. Liu, S. Okamoto, M. Van Veenendaal, M. Kareev, B. Gray, P. Ryan, J. Freeland, and J. Chakhalian, "Quantum confinement of mott electrons in ultrathin $LaNiO_3/LaAlO_3$ superlattices," *Physical Review B* **83**(16), p. 161102, 2011.

[37] T. Kim, D. Puggioni, Y. Yuan, L. Xie, H. Zhou, N. Campbell, P. Ryan, Y. Choi, J.-W. Kim, J. Patzner, *et al.*, "Polar metals by geometric design," *Nature* **533**(7601), pp. 68–72, 2016.

[38] B. Chen, N. Gauquelin, R. J. Green, J. H. Lee, C. Piamonteze, M. Spreitzer, D. Jannis, J. Verbeeck, M. Bibes, M. Huijben, *et al.*, "Spatially controlled octahedral rotations and metal-insulator transitions in nickelate superlattices," *Nano letters* **21**(3), pp. 1295–1302, 2021.

[39] J. Abraham and B. Deviot, "Resistivite d'un niobium de haute purete de 20 ka la temperature de fusion," *Journal of the Less Common Metals* **29**(3), pp. 311–320, 1972.

[40] D. Li, K. Lee, B. Y. Wang, M. Osada, S. Crossley, H. R. Lee, Y. Cui, Y. Hikita, and H. Y. Hwang, "Superconductivity in an infinite-layer nickelate," *Nature* **572**(7771), pp. 624–627, 2019.

[41] H. Takagi, B. Batlogg, H. Kao, J. Kwo, R. J. Cava, J. Krajewski, and W. Peck Jr, "Systematic evolution of temperature-dependent resistivity in $La_{2-x}Sr_xCuO_4$," *Physical review letters* **69**(20), p. 2975, 1992.

[42] A. Hebard, T. Palstra, R. Haddon, and R. Fleming, "Absence of saturation in the normal-state resistivity of thin films of K_3C_{30} and Rb_3C_{30}," *Physical Review B* **48**(13), p. 9945, 1993.

[43] T. Watanabe, T. Fujii, and A. Matsuda, "Anisotropic resistivities of precisely oxygen controlled single-crystal $Bi_2Sr_2CaCu_2O_{8+\delta}$: Systematic study on"spin gap"effect," *Physical review letters* **79**(11), p. 2113, 1997.

[44] Y. Nakajima, T. Metz, C. Eckberg, K. Kirshenbaum, A. Hughes, R. Wang, L. Wang, S. R. Saha, I.-L. Liu, N. P. Butch, *et al.*, "Quantum-critical scale invariance in a transition metal alloy," *Communications Physics* **3**(1), pp. 1–8, 2020.

[45] R. DS, L. JM, and D. RC, "Electrical resistivity of single crystal CrO_2," *Journal of the Physical Society of Japan* **21**(11), pp. 2430–2430, 1966.

[46] A. Tyler, A. Mackenzie, S. NishiZaki, and Y. Maeno, "High-temperature resistivity of $Sr_2RuO_4$4: Bad metallic transport in a good metal," *Physical Review B* **58**(16), p. R10107, 1998.

[47] P. B. Allen, R. M. Wentzcovitch, W. W. Schulz, and P. C. Canfield, "Resistivity of the high-temperature metallic phase of VO_2," *Physical Review B* **48**(7), p. 4359, 1993.

[48] Y. Maeno, H. Hashimoto, K. Yoshida, S. Nishizaki, T. Fujita, J. Bednorz, and F. Lichtenberg, "Superconductivity in a layered perovskite without copper," *Nature* **372**(6506), pp. 532–534, 1994.

[49] S. P. Lewis, P. B. Allen, and T. Sasaki, "Band structure and transport properties of cro 2," *Physical Review B* **55**(16), p. 10253, 1997.

[50] P. Giraldo-Gallo, J. Galvis, Z. Stegen, K. A. Modic, F. Balakirev, J. Betts, X. Lian, C. Moir, S. Riggs, J. Wu, *et al.*, "Scale-invariant magnetoresistance in a cuprate superconductor," *Science* **361**(6401), pp. 479–481, 2018.

[51] L. Taillefer, "Scattering and pairing in cuprate superconductors," *Annu. Rev. Condens. Matter Phys.* **1**(1), pp. 51–70, 2010.